The first principles study on the TbP compound

Y.O. Ciftci[A]*, Y. Mogulkoc[B] and M. Evecen[C]

***Abstract*—** The structural, elastic, electronic, thermodynamic and vibrational properties of TbP which crystallize in NaCl (B1), CsCl (B2), ZB (B3), tetragonal (L10), WC (Bh), NiAs (B8), PbO (B10) and wurtzite (B4) structures were analyzed by performing ab-initio calculations based on density functional theory using the Vienna Ab initio Simulation Package (VASP). The exchange correlation potential within the generalized-gradient apraximation (GGA) of projected augmented plane-wave (PAW) was used. The calculated structural parameters, such as the lattice constant, bulk modulus and its pressure derivative and formation energy and second-order elastic constants were presented for all calculated phases. This compound exhibits crystallographic phase transition from B1 to B2 phase at pressure 55 GPa. We have performed the thermodynamics properties for TbP by using quasi-harmonic Debye model. We have also predicted the temperature and pressure variation of the volume, bulk modulus, thermal expansion coefficient, heat capacities and Debye temperatures in a wide pressure (0-50 GPa) and temperature ranges (0-2000 K) for NiAs structure. The electronic band calculations, total density of states (DOS) and partial DOS were also presented. The computed phonon dispersion curves based on the linear response method are predicted. The obtained results are compared with the available experimental studies.

***Keywords*—**elastic properties, electronic properties, thermodynamic properties, TbP, structural properties

I. Introduction

The rare-earth monopnictides have attracted the interests of many researchers due to their numerous physical properties like magnetic, elastic, thermodynamics and phonon properties [1-21]. Buschbeck et al. [1] reported on the first magnetization measurements on TbP and TbSb in magnetic fields as high as 140 kOe covering the range from

high to low temperatures. Petit et al. [2] predict an electronic phase diagram of the entire range of rare earth monopnictides and monochalcogenides, composed of metallic, semiconducting and heavy fermion-like regions and exhibiting valency transitions brought about by a complex interplay between ligand chemistry and lanthanide contraction. Pagare et al. [3] report the high pressure behavior, electronic and elastic properties of two lutetium compounds, namely, LuAs and LuSb which crystallize in NaCl structure, by using density functional theory. J. Schoenes et al. [12] have studied optical properties of dysprosium monopnictides and presented their experimental and theoretical results. It is known that the source of these anomalous arise from the presence of 4f level close to the Fermi level [13]. Rare-earth elements are chemically very similar owing to an almost identical outer electron arrangement. Duan et al. [14] reviewed the electronic structures and magnetic properties of many rare-earth monopnictides. Because of the fully localized nature of the 4f electrons, the direct f-f interactions between neighbouring rare-earth atoms are typically considered to be closely negligible [14-16]. The earliest ab-initio electronic structure calculation of the rare-earth monopnictides was carried out by Hasegawa and Yanase in 1977 [17]. There are only some papers about TbAs and TbSb monopnictides. Nakanishi et al. [18] have investigated the Fermi surface (FS) and magnetic properties of rare-earth monopnictide TbSb by means of de Haas–van Alphen (dHvA) and high-field magnetization measurements. Nakanishi et al. [19] have investigated the magnetic and elastic properties of rare-earth monopnictide TbSb by means of specific heat, high-field magnetization, and ultrasonic measurements. Gordienko [20] has studied enthalpies of atomization and formation for some monopnictides. We have predicted structural, electronic, elastic, thermodynamic and vibration characteristics of TbN, using density functional theory within generalized-gradient (GGA) apraximation [21]. The TbP compound has not been studied very intensively and deeply using the first principle methods. Terbium phosphide (TbP) is an intermetallic compound of simple rocksalt structure. After the discovery of the transition to type-II antiferromagnetism the magnetic and elastic properties of TbP have attracted considerable experimental and theoretical interest [22]. The aim of the present paper is to reveal bulk, structural properties in B1, B2, B3, Bh, $L1_0$, B8, B10 and B4 structures and thermodynamical, electronic and elastic properties for TbP using first principles method with plane-wave pseudopotential. Method of calculation is given with some formulas in section 2. The obtained results are given with tables and figures in section 3. In last section, results and discussion are presented.

.

F. A. Author is with Gazi University, Department of Physics, Teknikokullar, 06500, Ankara, TURKEY(corresponding author to provide phone: +903122021266; e-mail: yasemin@gazi.edu.tr).

S. B. Author, Jr., was with [2]Ankara University, Department of Physics Engineering, 06100, Ankara, TURKEY (e-mail: yesim.mogulkoc @ eng.ankara.edu.tr).

T. C. Author is with [3]Amasya University, Department of Physics, Faculty of Arts and Sciences, 05000, Amasya, TURKEY (e-mail: meryem.evecen@amasya.edu.tr).

II. METHOD OF CALCULATION

In the present work, all the calculations have been carried out using the VASP [23-25] based on the density functional theory (DFT). The electron-ion interaction was considered in the form of the projector-augmented-wave (PAW) method [25, 26] with plane wave up to an energy of 500 eV for B1, B2, B3 structures, 600 eV for $L1_0$, B10 structures and 550 eV for Bh, B8 and B4 structures. This cut-off was found to be adequate for the structural, elastic properties as well as for the electronic structure. Any significant changes are not found in the key parameters when the energy cut-off is increased. For the exchange and correlation terms in the electron-electron interaction, Perdew and Zunger-type functional [27, 28] is used within the generalized gradient approximation (GGA) [26]. The *k*-point meshes for Brillouin zone sampling is constructed using the Monkhorst-Pack scheme [29]. The *12x12x12* for B1, B2 and B3 structures, *11x11x13* for $L1_0$ structure, *13x13x14* for Bh structure, *14x14x11* for B10 structure, *15x15x11* for B8 structure and *13x13x8* for B4 structure Monkhorst and Pack [29] grid of k-points have been used for integration in the irreducible Brillouin zone. Thus, this mesh ensures a convergence of total energy to less than 10^{-5} ev/atom.

The thermodynamic properties of TbP are calculated by GIBBS program. The GIBBS code is used to investigate isothermal-isobaric thermodynamics of a compound from energy curves via quasi-harmonic Debye model [30] is used to obtain the thermodynamic properties of TbP in which the non-equilibrium Gibbs function *G*(V; P, T)* takes the form of

$$G^*(V;P,T) = E(V)+PV+A_{vib}[\theta(V);T] \quad (1)$$

In Eq.(1), *E(V)* is the total energy for per unit cell of TbP, *PV* corresponds to the constant hydrostatic pressure condition, $\theta(V)$ the Debye temperature and A_{Vib} is the vibration term, which can be written using the Debye model of the phonon density of states as

$$\mathrm{A_{Vib}}(\theta,\mathrm{T}) = nkT\left[\frac{9\theta}{8T}+3\ln\left(1-e^{-\frac{\theta}{T}}\right)-D\left(\frac{\theta}{T}\right)\right] \quad (2)$$

(2)

where *n* is the number of atoms per formula unit, $D\left(\frac{\theta}{T}\right)$ the Debye integral, and for an isotropic solid, θ is expressed as [31]

$$\theta_D = \frac{\hbar}{k}\left[6\pi V^{1/2}n\right]^{1/3} f(\sigma)\sqrt{\frac{B_s}{M}} \quad (3)$$

where *M* is the molecular mass per unit cell and B_S the adiabatic bulk modulus, which is approximated given by the static compressibility [32]:

$$B_s \approx B(V) = V\frac{d^2E(V)}{dV^2} \quad (4)$$

$f(\sigma)$ is given by Refs. [31-33] and the Poisson ratio is used as 0,2070 and *n*=4 *M*= 189.904 for TbP. Therefore, the non-equilibrium Gibbs function *G*(V; P, T)* as a function of *(V; P, T)* can be minimized with respect to volume *V*.

$$\left[\frac{\partial G^*(V;P,T)}{\partial V}\right]_{P,T} = 0 \quad (5)$$

By solving Eq. (5), one can obtain the thermal equation of state (EOS) *V(P, T).* The heat capacity at constant volume $C_{V,}$ the heat capacity at constant pressure C_p, the entropy S and the thermal expansion coefficient α are given [34] as follows:

$$C_v = 3nk\left[4D\left(\frac{\theta}{T}\right)-\frac{3\theta/T}{e^{\theta/T}-1}\right] \quad (6)$$

$$S = nk\left[4D\left(\frac{\theta}{T}\right)-3\ln(1-e^{-\theta/T}\right] \quad (7)$$

$$\alpha = \frac{\gamma C_v}{B_T V} \quad (8)$$

$$C_p = C_v(1+\alpha\gamma T) \quad (9)$$

Here γ represent the Grüneisen parameter and it is expressed as

$$\gamma = -\frac{d\ln\theta(\mathrm{V})}{d\ln \mathrm{V}}\ . \quad (10)$$

III. RESULTS AND DISCUSSION

Structural and electronic properties

Firstly, the equilibrium lattice parameter has been computed by minimizing the crystal total energy calculated for different values of lattice constant by means of Murnaghan's equation of state (EOS) [35] as in Figure 1. In addition, from the EOS curves as shown in Figure 1, it can be seen that in the low volume region the B8 structure is energetically favorable between inversitigated eight structures.

The bulk modulus and its pressure derivative have also been calculated based on the same Murnaghan's equation of state and the results are given in Table 1 along with the experimental and other theoretical values. The calculated values of lattice parameter are 5.6960 Å in NaCl (B1) structure, 3.484 Å in CsCl (B2) structure, 6.3143 Å in ZB

(B3) structure, 4.7295 Å in tetragonal ($L1_0$) structure, 3.9145 Å in WC (Bh) structure, 4.0787 Å in NiAs (B8) structure, 5.1220 Å in PbO (B10) structure and 4.4784 Å in wurtzite (B4) structure for TbP. The NiAs (B8) structure of TbP is determined as stable phase in this study. The present values for lattice constants are also listed in Table 1 and the obtained results are quite accord with the other experimental values [36-40]. The present lattice constant in B1 structure for TbP is nearly 0.084% higher than the reference experimental values [36-40].

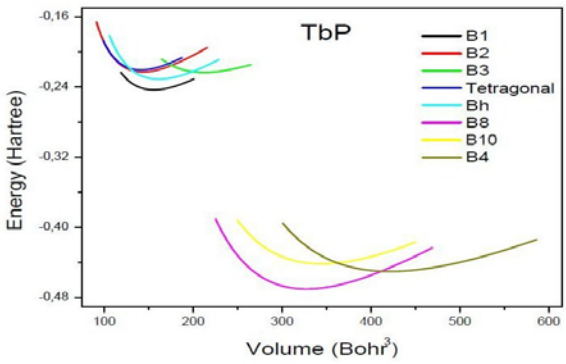

Fig. 1. Energy-volume curves for all calculated structures of TbP.

Table1. Calculated equilibrium lattice constants (a_0), bulk modulus (B), pressure derivatives of bulk modulus (B'), formation enthalpy (ΔH) and other theoretical works for TbP in structures

Structure	Reference	a	c	c/a	B(GPa)	B'	ΔH (eV/atom)
B1	Present	5.696			84.2160	3.8253	2.82451
	Exp.	5.686[a]					
	Exp.	5.600[b]					
	Exp.	5.690[c]					
	Exp.	5.690[d]					
	Exp.	5.688[e]					
B2	Present	3.484			82.40567	3.7808	3.92183
B3	Present	6.3143			55.11767	3.6574	3.91157
Bh	Present	3.9145	3.5907	0.9173	76.8677	3.6387	3.48817
$L1_0$	Present	4.7195	3.7345	0.7913	4.20908	3.8602	4.05955
B8	Present	4.0787	6.7261	1.6491	78.0407	3.8147	-9.53615
B10	Present	5.1220	3.8906	0.7596	66.8960	3.6272	-7.96322
B4	Present	4.4784	7.1905	1.6056	54.0484	3.6740	-8.44314

[a] Ref. [36]. [b]Ref. [37]. [c] Ref. [38]. [d] Ref. [39]. [e] Ref. [40].

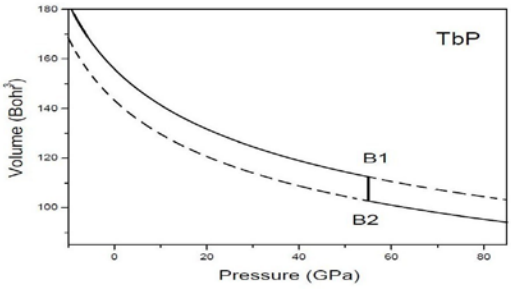

Fig. 2. Volume-pressure curves for B1 and B2 structures of TbP.

The thermodynamic stability of TbP compound in different structures can be reflected by the formation enthalpy (ΔH). Negative formation enthalpy means an exothermic process, and the lower formation energy indicates the stability with respect to the decomposition to elemental constituents. The formation enthalpy can be calculated by the following expression [41]:

$$\Delta H=(E_{top}-\sum n_i E_i)/n \quad (11)$$

where E_{tot} is the total energy of the bulk compound with n_i atoms of all i (Tb and P), n is the total number of atoms in the primitive cell, and E_i is the total energy of a pure $_i$ atom with equilibrium lattice parameters. The calculated theoretical formation enthalpies of TbP compounds are included in Table1. Unfortunately as far as it is known, there are no data available related to formation energy in the literature to compare with its. Negative formation enthalpies indicate their structural stabilities from energetic point of view. B8 structure of TbP shows the lowest value of formation enthalpy, which indicates that B8 structure of TbP has the highest structural stability which is compatible with Figure 1.

Our computational approach is based on constant-pressure static quantum mechanical calculations at T=0 K, so the relative stability of different phases can be deduced from the pressure dependence of the enthalpy instead of the Gibbs free energy [42]. The pressure-volume curve is plotted for both B1 and B2 structures of TbP in Figure 2. Naturally, the cell volume decreases with increasing pressure values. The

discontinuity in volume takes place at the phase transition pressure. The phase transition pressures from B1 to B2 structure are found to be 55 GPa TbP.

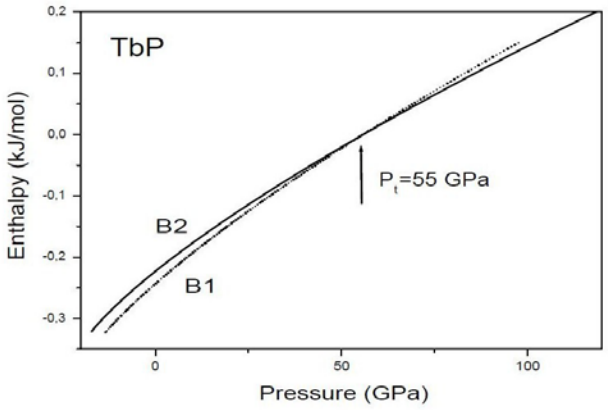

Fig. 3. Enthalpy-pressure curves for B1 and B2 structures of TbP

The related enthalpy versus pressure graph is shown in Figure 3 for TbP. The transition pressure is a pressure at which H(p) curves for both structures cross. The same result is also confirmed in terms of the common tangent technique in Figure 1.

In order to understand the electronic and phase stability of TbP the energy band structure along with total electronic density of states at 0 GPa for B8 are presented in Figure 4. Fermi level is set 0eV. Our calculation shows that the B8 structure of TbP is of metallic conductivity as there is no band gap near the Fermi level and there are many bands crossing the Fermi level.

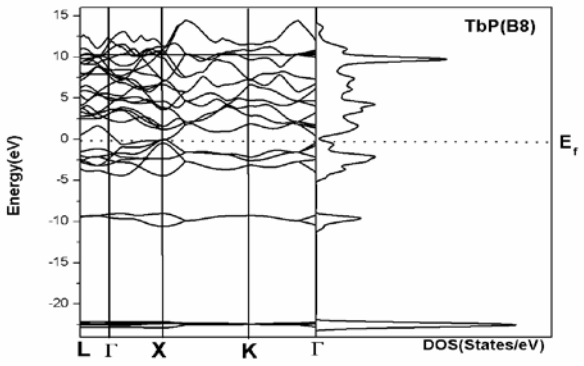

Fig. 4. Electronic band structure and total density of states of TbP(B8).

(a)

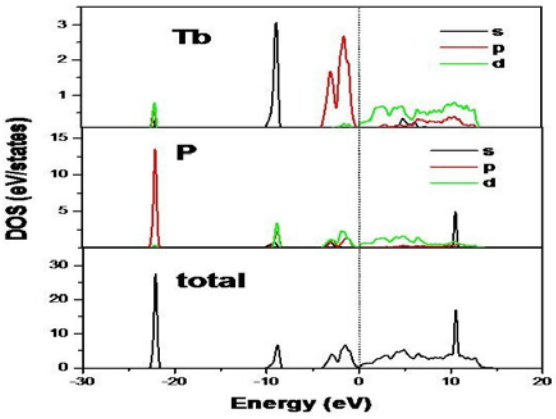

(b)

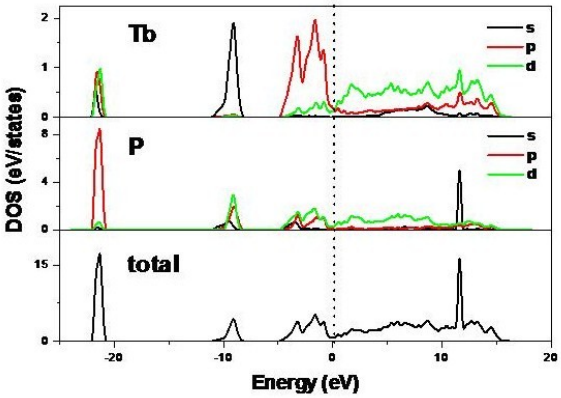

Fig. 5. Partial and total DOS of TbP(B8) at (a) 0 GPa (b)50GPa

Partial DOS figures are also presented at 0 GPa and 50 GPa for TbP in B8 structure in Figure 5. The lowest valance bands occur between about -10.5 and 5.5 eV are essentially dominated by Tb-s states. Other valance bands are essentially dominated by Tb-p, Tb-d, P-p and P-d states. In Fig. 5 (b), the lowest valance bands occur between about -11 and 12 eV are dominated by Tb-s states. Tb-d and P-d states are more robust at 50 GPa according to 0 GPa. Contribution of the P-p state at 0 GPa is more than at 50 GPa.

Elastic properties

Elastic properties of materials are very important because of various fundamental solid state properties, such as Zener anisotropy factor, shear modulus, Poisson's ratio, Young modulus and so on. The elastic constants determine the response of the crystal to external forces and play a big role in determining the strength of the materials.

There are two common methods [43, 44] for obtaining the elastic constants through the ab-initio modelling of materials from their known crystal structures: an approach based on analysis of the total energy of properly strained states of the material in the volume conserving technique and an approach based on the analysis of changes in calculated stress values resulting from changes in the stress-strain technique. In this

work, the stress-strain technique is used for obtaining the second-order elastic constants (C_{ij}). The stress-strain technique is based on constructing a set of linear equations from stress–strain relation for several deformations of the unit cell. This set of equations represents a general form of Hook's law and can be solved with respect to the elastic constants.

$$\sigma_i = \sum_{J=1}^{6} C_{ij}\varepsilon_j \ , \qquad (11)$$

that describes the linear dependency of stress component σ_i (i = 1–6) and applied strain ε_j (j = 1–6) under a small deformation. Here C_{ij} are the elastic constants of the crystal whose structure has been fully relaxed under a given set of exchange–correlation potential functions and attained an equilibrium structure with a minimum total energy. In order to obtain the elastic constants, we calculate the second derivatives of the internal energy with respect to the strain tensor. The Born's stability criteria's [45] should be satisfied for the stability of lattice. The known conditions for mechanical stability of cubic crystals are: $C_{11}>0$, $C_{11}-C_{12}>0$, $C_{44}>0$, $C_{11}+2C_{12}>0$ and $C_{12}<B<C_{11}$. For hexagonal structure the mechanical stability criteria are given by $C_{44}>0$, $C_{11}>C_{12}$, $(C_{11}+2C_{12})C_{33}>2C_{13}^2$. For tetragonal structure the mechanical stability criteria are $C_{11}>0$, $C_{33}>0$, $C_{44}>0$, $C_{66}>0$, $(C_{11}-C_{12})>0$, $(C_{11}+C_{33}-2C_{12})>0$ and $2(C_{11}+C_{12})+C_{33}+4C_{13}>0$.

Table 2. The calculated elastic constants (in GPa unit) in different structures for TbP.

Structure	Reference	C_{11}	C_{12}	C_{44}	C_{33}	C_{13}	C_{66}	Stability
B1	Present	211.06	26.81	45.56				*Stable*
B2	Present	151.16	55.15	38.63				*Stable*
B3	Present	60.54	54.01	39.78				*Stable*
Bh	Present	139.56	51.34	44.11	207.57	35.38	19.00	*Stable*
$L1_0$	Present	13.89	166.98	41.64	173.20	62.91	39.09	*Unstable*
B8	Present	147.14	44.95	51.10	197.81	40.51	56.66	*Stable*
B10	Present	180.30	64.34	52.77	42.80	23.61	6.69	*Stable*
B4	Present	97.99	41.63	28.19	114.65	29.74	20.40	*Stable*

The calculated values of C_{ij} are given in Table 2 for TbP compound. The related mechanical stability conditions are satisfied except for $L1_0$ structure in TbP. The $L1_0$ structure in TbP is mechanically unstable despite the fact that all other structures in TbP are mechanically stable. For cubic structures (B1, B2 and B3) C_{11} are higher than C_{12} and C_{44} and other structures, the values of C_{11} and C_{33} are much higher than those of C_{12}; C_{13}; C_{44} and C_{66}, indicating TbP compound under investigation is mechanically anisotropic and the shear deformation is easier to take place than compression deformations along the principle direction a- and c-axis. To our best knowledge, no experimental and theoretical data are available in the literature to be compared with our results. Then, our results can serve as a prediction for future investigations.

The Zener anisotropy factor *A*, Poisson's ratio υ, and Young's modulus *Y*, which are the most interesting elastic properties for applications, are also calculated in terms of the computed using the following relations [46]:

$$A = \frac{2C_{44}}{C_{11}-C_{12}}, \qquad (12)$$

$$\upsilon = \frac{1}{2}\left[\frac{(B-\frac{2}{3}G)}{(B+\frac{1}{3}G)}\right], \qquad (13)$$

$$Y = \frac{9G\ B}{G+3B} \qquad (14)$$

where $G=(G_V+G_R)/2$ is the isotropic shear modulus, G_V is Voigt's shear modulus corresponding to the upper bound of G values and G_R is Reuss's shear modulus corresponding to the

lower bound of G values and can be written as $G_V=(C_{11}-C_{12}+3C_{44})/5$ and $5/G_R= 4/(C_{11}-C_{12})+3/C_{44}$. The calculated Zener anisotropy factor (A), Poisson ratio (υ), Young's modulus (Y) and Shear modulus ($C'= (C_{11}-C_{12}+2C_{44})/4$) for TbP are given in Table 3 and they are close to these obtained for the similar structural symmetries.

Table 3. The calculated Zener anisotropy factor (A), Poisson's ratio (υ), Young's modulus (Y), shear modulus (C') for TbP in B8 phase.

Material	A	υ	Y (GPa)	C' (GPa)	B/G
TbP	1	0.2070	137.17	51.10	1.53

The Zener anisotropy factor (A) takes the value of 1 for a completely isotropic material that shows this compound is completely isotropic materials. The Poisson's ratio (υ) characterizes the stability of the crystal against shearing strin. For a typical metal, the value is supposed to be 0.33; for the ionic-covalent crystal, the value is to be between 0.2 and 0.3. We obtain 0.207 that is situated ionic-covalent crystal. The Young modulus (Y) which is calculated 137.17 GPa is measurement of the stiffness of the solids. B/G ratios that are roughly as a measurement of brittlement or ductility are also given in Table 3. Providing that the critical value is 1.75 and/or more than this value, the material is regarded as ductile. [47-49]. TbP in B8 structure indicates britttle behavior due to the fact that the present value of B/G is 1.53. As seen form table 3, the values of B/G ratio for TbP compound ise smaller than the critical value, thus this compounds in B8 structure may be classified as brittle material. Mechanical properties such as ductility and brittleness of semiconductor materials are very important for their technological applications.

Thermodynamic properties

Thermodynamic properties are determined in the temperature range 0-2000 K and the pressure range 0-50 GPa for B8 structure of TbP. The calculations based on the first principles methods demonstrate that quasi-harmonic approximation provides a reasonable description of the dynamic properties of many bulk materials below the melting point [50-54]. The melting point of TbP is calculated to be 1422±300 K. Hence, for decreasing the probable influence of anharmonicity, where the quasi-harmonic model remains fully valid. The Debye temperature (θ_D) is known as an important fundamental parameter closely related to many physical properties such as specific heat and melting temperature. At low temperatures the vibrational excitations arise solely from acoustic vibrations. Hence, at low temperatures the Debye temperature calculated from elastic constants is the same as that determined from specific heat measurements. We have calculated the Debye temperature, θ_D, from the elastic constants using the average sound velocity, v_m, by the following common relation given [55]

$$\theta_D = \frac{h}{k}\left[\frac{3n}{4\pi}\left(\frac{N_A\rho}{M}\right)\right]^{1/3}\upsilon_m \qquad (15)$$

where $\hbar$ is Planck's constants, k is Boltzmann's constants, N_A Avogadro's number, n is the number of atoms per formula unit, M is the molecular mass per formula unit, $\rho(=M/V)$ is the density, and v_m is obtained from

$$\upsilon_m = \left[\frac{1}{3}\left(\frac{2}{\upsilon_t^3}+\frac{1}{\upsilon_l^3}\right)\right]^{-1/3} \qquad (16)$$

where v_l and v_t, are the longitudinal and transverse elastic wave velocities, respectively, which are obtained from Navier's equations [56]:

$$\upsilon_l = \sqrt{\frac{3B+4G}{3\rho}} \qquad (17)$$

and

$$\upsilon_t = \sqrt{\frac{G}{\rho}}\,. \qquad (18)$$

Table 4. The longitudinal (v_l), transverse (v_t), average (v_m) elastic wave velocities, Debye temperature (θ_D) and melting temperature (T_m) for TbP(B8).

Mater.	$\upsilon_l(m/s)$	$\upsilon_t(m/s)$	$\upsilon_m(m/s)$	$\theta_D(K)$	$T_m(K)$
TbP	6873.4	4177.8	4615.7	377.0	1422.6 ± 300

The calculated longitudinal, transverse and average elastic wave velocities, Debye temperature and melting temperature for TbP are given in Table 4. No other theoretical or experimental values are exist for comparison with these present values.

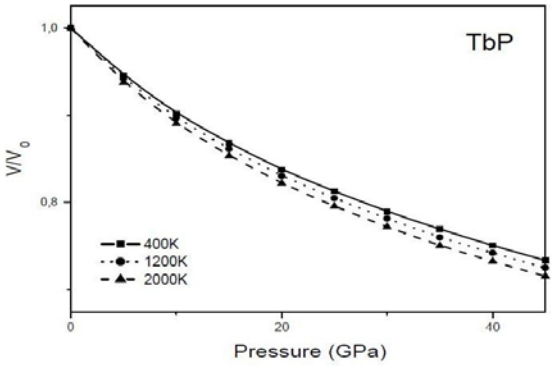

Fig. 6. The normalized volume-pressure curves for B8 structure of TbP at different temperatures

The relationship between normalized volume and pressure at different temperature is shown in Figure 6 for TbP. It can

be seen that when the pressure increases from 0 GPa to 50 GPa the volume decreases. The reason of this changing can be attributed to the atoms in the interlayer become closer, and their interactions become stronger.

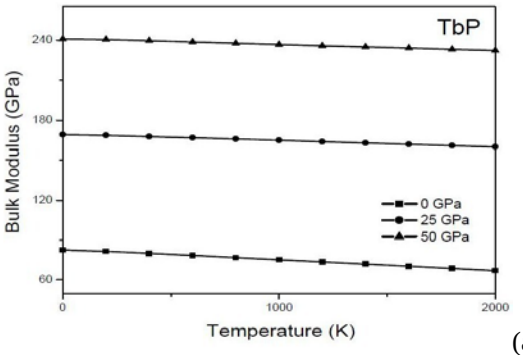

(a)

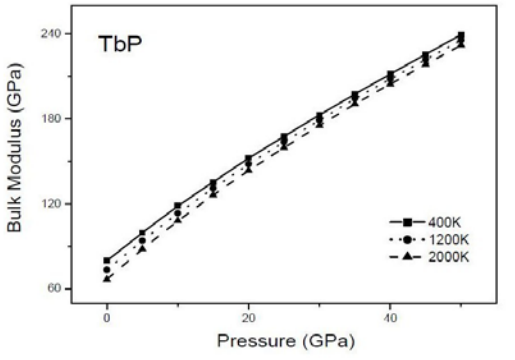

(b)

Figure 7. (a) The variations of bulk modulus with temperature for B8 structure of TbP.

(b) The variations of bulk modulus with pressure for B8 structure of TbP.

The variations of bulk modulus, B, with temperatures and pressures are presented in Fig. 7 for B8 structure. It can be easily seen that B decreases as temperature increases in Figure 7 (a). Because cell volume changes rapidly as temperature increases. Relations of bulk modulus and temperature polynomial curves are third-order fitted and performed for stable structure TbP(B8). Relation is given as below at 0 GPa for TbP.

$B = 82.65455 - 6.06 \times 10^{-3} T - 1.75699 \times 10^{-6} T^2 + 4.23951 \times 10^{-10} T^3$

The relationship between bulk modulus and pressure at different temperatures (400, 1200 and 2000K) is shown in Figure 7(b) for TbP. It can be seen that bulk modulus decreases with the temperature at a given pressure and increases with pressure at a given temperature. It shows that the effect of increasing pressure on TbP is the same as decreasing its temperature.

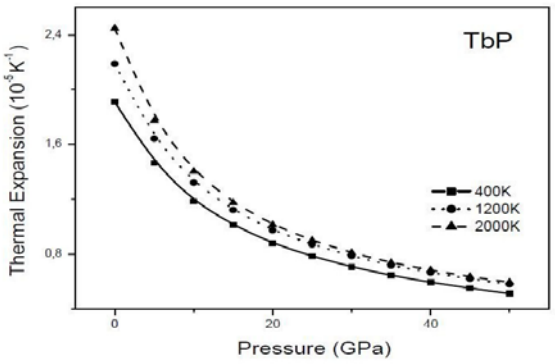

(a)

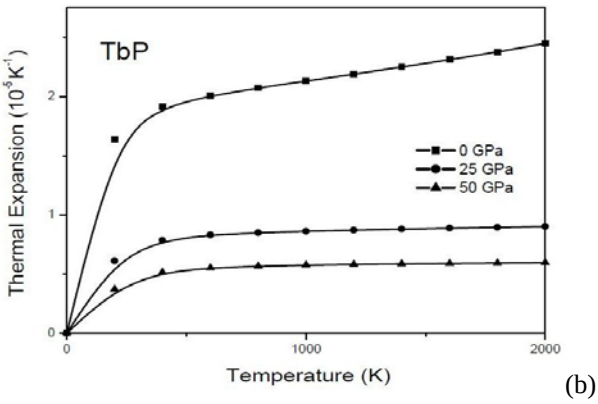

(b)

Figure 8.(a) The thermal expansion coefficient versus pressure at different temperatures for TbP in B8 structure.

(b) The thermal expansion coefficient versus temperature at different pressures for TbP in B8 structure.

The variations of the thermal expansion coefficient (α) with pressure and temperature are shown in Figure 8 for TbP. At different temperatures, thermal expansion coefficient decreases nonlinearly at lower pressure and decreases almost linearly at higher pressure values in Fig. 8(a). The thermal expansion coefficient increases at lower temperatures and gradually approaches linear increases at higher temperatures, while the thermal expansion coefficient decreases with pressure in Fig. 8(b).

ISBN: 978-1-61804-286-6

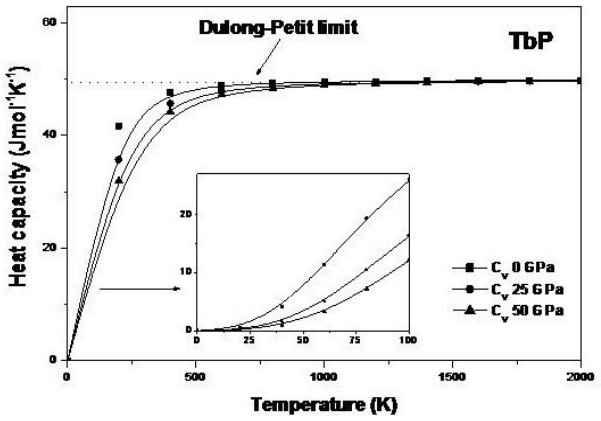

Fig. 9. The variation of C_v with temperature at different pressures for TbP.

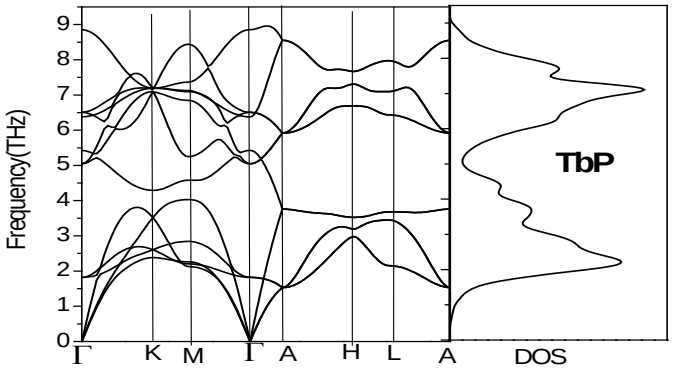

Fig. 10. The calculated phonon dispersions and density of states for TbP in B8 structure.

The variations of the temperature dependence of the heat capacity at constant volume, C_V, at different pressures, presented in Figure 9 for TbP follows the Debye Law that is at low temperatures (T<250 K), C_V is proportional to T^3 and high temperatures (T>500 K) the heat capacity C_V is very close to Dulong-Petit limit.

Phonon Dispersion Curves

The phonon dispersion curves and phonon density of states for B8 structure of TbP are calculated by using the PHONOPY program [57] using the interatomic force constants obtained from VASP [23-25] which is use linear response method within the density functional perturbation theory (DFPT) [58- 60]. The Phonopy program which is based on real space supercell calculates phonon frequencies from force constants. The obtained phonon dispersion curves and the corresponding one-phonon DOS for TbP along the high symmetry directions using a 2x2x2 cubic supercell of 32 atoms are illustrated in Fig. 10. The absence of the soft modes in the phonon dispersion curves confirms the dynamical stability of TbP. To our knowledge there are no experimental and other theoretical works exploring the lattice dynamics of this compound for comparison with the present data; hence our work is a first attempt in this direction. Owing to the mass difference between Tb and P atom the no band gap takes place between acoustic and optical regions. On the right side of phonon curves in Fig. 10, the corresponding total density of phonon states for this compound is shown.

IV. SUMMARY AND CONCLUSION

In our detailed work, we have investigated the structural, elastic, electronic and thermodynamic and vibrational properties properties of TbP in different structures using ab-initio plane wave pseudopotentials density functional theory (DFT). The lattice parameters are calculated and found good agreement with other experimental values for B1 structure. On the basis of using common tangent method, we have found that phase transition from B1 to B2 phase occurs at about 55 GPa for TbP. Electronic calculations are presented with band stuructures, total density of states and partial DOS. The electronic properties are performed both at 0 GPa and 50 GPa pressure values. The zero pressure second order elastic constants and their related quantities such as bulk modulus, shear modulus, Young's modulus, Zener anisotropy factor, Poisson ratio and B/G ratios are investigated and decided to brittle/ductile behavior for this compound which shows brittle behavior. The quasi-harmonic Debye model is successfully used for thermodynamic properties calculations in the wide range temperature and pressure values. The longitudinal, transverse, average elastic wave velocities, Debye temperatures and melting points for TbP in B8 structure are calculated and given in related tables. The absence of the soft modes in the phonon dispersion curves confirms the dynamical stability of TbP. To the best of our knowledge, our calculations are the first theoretical prediction on the thermodynamic

ACKNOWLEDGMENT

Acknowledgments Authors want to express their great acknowledges to the scientific research unit of Amasya University for the financial support to this study with Grant Number of FMB-BAP-13-059.

REFERENCES

[1] A. Buschbeck, G.H. Chojnowski, J. Kötzler, R. Sonder and G. Thummes, "Field-dependent phase transitions and magnetization of the type II- antiferromagnets TbP and TbSb", Journal of Magnetism and Magnetic Materials, vol. 69, Oct. 1987, pp. 171–182.

[2] L. Petit, R. Tyer, Z. Szotek, W.M. Temmerman and A. Svane, “Rare earth monopnictides and monochalcogenides from first principles: towards an electronic phase diagram of strongly correlated materials” New J. Phys. vol. 12, Nov. 2010 113041 (20pp).

[3] G. Pagare, S.S. Chouhan, P. Soni, S.P. Sanyal, M. Rajagopalan, “First principles study of structural, electronic and elastic properties of lutatium mono-pnictides” Comp. Maters. Sci. vol. 50, Dec. 2010 538-544.

[4] G. Bruzzone, A.F. Ruggiero, “The equilibrium diagram of the calcium-indium system” J. Less-Common Met. Vol. 7 Nov. 1964, 368–372.

[5] G. Bruzzone, "Sui sistemi binari Sr− Tl, Ba− Tl e Ca− Tl." Annali di Chimica, Rome vol. 56 1966, 1306–1319.

[6] J.D. Marcoll, P.C. Schmidt, A. Weiss, Z. Naturforsch, “X-Ray investigations of intermetallics phases CaCd1-XTlX and CaIn1-XTlX and knight-shift measurements of Tl-205-NMR and Cd-113-NMR in system CaCd1-XTlX.” Zeitschrift Fur Naturforschung Section AA J. Phys. Scienc. vol. 3, 1974, 473–476.

[7] J. Rosat-Mignod, J.M. Effantin, P. Burlet, T. Chattopadhyay, L.P. Regnault, H. Bartholin, C. Vettier, "0. Vogt, D. Ravot and JC Achard.", J. Magn. Magn. Mater. vol. 52, 1985, 111.

[8] T. Chattopadhyay, P. Burlet, J. Rosat-Mignod, H. Bartholin, C. Vettier, and O. Vogt, “High-pressure neutron and magnetization investigations of the magnetic ordering in CeSb” Phys. Rev. B vol. 49, Jun. 1994, 15096.

[9] R. Pittini, J. Schoenes, O. Vogt, and P. Wachter, “Discovery of 90 degree Magneto-optical Polar Kerr Rotation in CeSb” Phys. Rev. Lett. vol.77, Jul. 1996, 944.

[10] R. Pittini, J. Schoenes, F. Hulliger, and P. Wachter, “Periodicity of the Spin Structure Observed in the Optical Response of CeBi Single Crystals” Phys. Rev. Lett. vol. 76, Apr. 1996, 3428.

[11] O. Vogt and K. Mattenberger, “The extraordinary case of CeSb” Physica B: Cond. Matt. vol. 215, Oct. 1995, 22-26.

[12] J. Schoenes, P. Repond, F. Hulliger, D.B. Ghosh, S.K. De, J. Kunes, P.M. Oppeneer, “Experimental and theoretical investigation of optical properties of dysprosium monopnictides” Phys. Rev. B vol. 68, Aug. 2003, 085102.

[13] E. Zintl, C. Brauer, Z. Phys. Chem., Abt. B vol. 20 1933, 245–271.

[14] Chun-Gang Duan, R.F. Sabirianov, W.N. Mei, P.A. Dowben, S.S. Jaswall and E.Y. Tsymbal, “Electronic, magnetic and transport properties of rare-earth monopnictides” Journal of Physics: Condensed Matter vol.19, Jul. 2007, 315220.

[15] E. Zintl, S. Neumayr, “Gitterstruktur des Indiums. (7. Mitteilung über Metalle und Legierungen)”Z. Elektrochem. vol. 39, Febr. 1933, 81-84.

[16] B.D. Cullity, Introduction to Magnetic Materials, , in: M. Cohen Ed. , Addison-Wesley Publishing, Reading, Mas- Ž . sachusetts, 1972, p. 178.

[17] A. Hasegawa and A. Yanase, “Energy Band Structures of Gd-Pnictides” J. Phys. Soc. Japan, vol. 42, 1977, 492-498.

[18] Y. Nakanishi, T. Sakon, M. Motokawa, T. Suzuki, “De Haas–van Alphen study of the spin splitting of the Fermi surface in TbSb” Phys. Rev. B vol. 69, Jun. 2004, 024412-6.

[19] Y. Nakanishi, T. Sakon, M. Motokawa, T. Suzuki, M. Yoshizawa, “Elastic properties and phase diagram of the rare-earth monopnictide TbSb” Phys. Rev. B vol. 69, Oct. 2003, 144427-6.

[20] S.P. Gordienko, “Reaction of Titanium with Boron Nitride under Self-Propagating High-Temperature Synthesis Conditions” Powder Metallurgy and Metal Ceramics, vol. 40, Jan. 2001, 58-60.

[21] Y.O. Ciftci, M. Ozayman, G. Surucu , K. Colakoglu, E. Deligoz, “Structural, electronic, elastic, thermodynamic and vibration properties of TbN compound from first principles calculations” Solid State Sciences vol.14, Mar. 2012, 401-408.

[22] J. Kötzler, G. Raffius, A. Loidl and C.M.E. Zeyen, “Singlet-groundstate magnetism in TbP” Z. Physik, B vol. 35, May. 1979, 125-132.

[23] G. Kresse and J. Hafner, “Ab. initio molecular dynamics for liquid metals” Phys. Rev. B vol. 47, Jan. 1993, 558-561.

[24] G. Kresse and J. Furthmauller, “Efficient iterative schemes for ab initio total-energy calculations using a plane-wave basis set” Phys. Rev. B vol. 54, Oct. 1996, 11169-11186.

[25] G. Kresse and D. Joubert, “From ultrasoft pseudopotentials to the projector augmented-wave method” Phys. Rev. B vopl. 59, Jan. 1999, 1758-1775.

[26] P.E. Blochl, “Projector augmented-wave method” Phys. Rev. B vol. 50, Dec. 1994, 17953-17979.

[27] J.P. Perdew and A. Zunger, “Self-interaction correction to density-functional approximations for many-electron systems” Phys. Rev. B vol. 23, May. 1981, 5048-5079.

[28] J.P. Perdew, J.A. Chevary, S.H. Vosko, K.A .Jackson, M.R. Pederson, D.J. Singh and C. Fiolhais, “Atoms, molecules, solids, and surfaces: Applications of the generalized gradient approximation for exchange and correlation” Phys. Rev. B vol. 46, Sep. 1992, 6671-6687.

[29] H.J. Monkhorst and J.D. Pack, “Special points for Brillonin-zone integrations” Phys. Rev. B, vol. 13, Jun. 1976 5188-5192.

[30] M.A. Blanco, E. Francisco, V. Lunana, “GIBBS: isothermal-isobaric thermodynamics of solids from energy curves using a quasi-harmonic Debye model” Comput. Phys. Commun. vol. 158, Marc. 2004, 57-72.

[31] M.A. Blanco, A.M. Pendàs, E. Francisco, J.M. Recio, R. Franko, “Thermodynamical properties of solids from microscopic theory: applications to MgF_2 and Al_2O_3” J.Mol. Struct. (Theochem) vol. 368, Sep. 1996, 245-255.

[32] M. Flórez, J.M. Recio, E. Francisco, M.A. Blanco, A.M. Pendàs, “First-principles study of the rocksalt–cesium chloride relative phase stability in alkali halides” Phys. Rev. B vol. 66, Oct. 2002, 144112-8.

[33] E. Francisco, J.M. Recio, M.A. Blanco, A.M. Pendàs, “Quantum-Mechanical Study of Thermodynamic and Bonding Properties of MgF_2” J. Phys. Chem. vol.102, (1998) 1595-1601.

[34] R. Hill, “The Elastic Behaviour of a Crystalline Aggregate” Proc. Phys. Soc. Lond. A vol. 65, 1952, 349-354.

[35] F.D. Murnaghan, Proc. Natl., Acad. Sci. USA vol. 30, 1944, 5390.

[36] F. Lévy F, Phys. Kondens. Mater. vol. 10, 1969, 85–106.

[37] K. Yaguchi, J. Phys. Soc. Jpn. vol. 21, 1996, 1226.

[38] H.R Child, M.K. Wilkinson, J.W. Cable, W.C. Koehler, E.O. Wollan, “Neutron Diffraction Investigation of the Magnetic Proyerties of Cornyounds of Rare-Earth Metals with Grouy V Anions” Phys. Rev. vol. 131, Aug. 1963, 922–931.

[39] M.K. Wilkinson, H.R Child, W.C. Koehler, J.W. Cable, E.O. Wollan, “"Recent Magnetic Neutron Scattering Investigations at Oak Ridge National Laboratory" J. Phys. Soc. Jpn. vol. 17, 1962, 27–31.

[40] G.L. Olcese, G.B. Bonino, Atti Accad. Naz. Lincei, Cl. Sci. Fis., Mat. Nat., Rend. vol. 30 1961, 195–200.

[41] Y.P. Xie, Z.Y. Wang, Z.F. Hou, “The phase stability and elastic properties of $MgZn_2$ and Mg_4Zn_7 in Mg–Zn alloys” Scr. Mater. vol. 68, Apr. 2013, 495-498.

[42] A. Hao, Y. Zhu, “First-principle investigations of structural stability of beryllium under high pressure” J. Appl. Phys. vol.112, Jul. 2012, 023519-4.

[43] J. Mehl, “Pressure dependence of the elastic moduli in aluminum-rich Al-Li compounds” Phys. Rev. B vol. 47, Feb. 1993, 2493-2500.

[44] S.Q. Wang, H.Q. Ye, **“**First-principles study on elastic properties and phase stability of III–V compounds” Phys. Status Solidi B vol. 240, 2003, 45-54.

[45] M. Born and K. Huang, Dynamical Theory of Crystal Lattices, Clarendon, Oxford, 1956.

[46] B. Mayer, H. Anton, E. Bott, M. Methfessel, J. Sticht, and P. C. Schmidt, “Ab-initio calculation of the elastic constants and thermal expansion coefficients of Laves phases” Intermetallics vol. 11, Jan. 2003, 23-32.

[47] S.F. Pugh, “XCII. Relations between the elastic moduli and the plastic properties of polycrystalline pure metals” Phil. Mag. vol. 45, Apr. 1954, 823-843.

[48] V.V. Bannikov, I.R. Shein, A.L. “Electronic structure, chemical bonding and elastic properties of the first thorium-containing nitride perovskite $TaThN_3$” Ivanovskii Phys Status Solidi (RRL) vol. 1, May. 2007, 89-91.

[49] I. Johnston, G.Keeler, R. Rollins, and S.Spicklemire, Solid State Physics Simulations, The Consortium for Upper-Level Physics Software, John Wiley, New York, 1996.

[50] S. Biernacki, M. Scheffler, “Negative Thermal Expansion of Diamond and Zinc-Blende Semiconductors” Phys. Rev. Lett. vol.63 Jul. 1989, 290-293.

[51] A. Fleszar, X. Gonze, “First-principles thermodynamical properties of semiconductors” Phys. Rev. Lett. vol. 64, Jun. 1990, 2961.

[52] P. Pavone, K. Karch, O. Schutt, W. Windl, D. Strauch, P. Giannozzi, S. Baroni, “Ab initio lattice dynamics of diamond” Phys. Rev. B vol. 48, Aug. 1993, 3156-3163.

[53] P. Pavone, S. Baroni, S. De Gironcoli, “a↔b phase transition in tin: A theoretical study based on density-functional perturbation theory” Phys. Rev. B vol. 48, May. 1998, 10421-10423.

[54] A.A. Quang, A.Y. Liu, “First-principles calculations of the thermal expansion of metals” Phys. Rev. B vol. 56, Oct. 1997, 7767-7770.
[55] E. Schreiber, O. L. Anderson, N. Soga, Elastic Constants and Their Measurements, McGraw-Hill, New York, 1973.
[56] M.E. Fine, L.D. Brown, H.L. Marcus, Scr. Metall. vol.18, 1984, 951.
[57] A. Togo, F. Oba, and I. Tanaka, Phys. Rev. B, vol. 78, 2008, 134106-1-9.
[58] S. Baroni, P. Giannozzi, and A. Testa “Green′s-function approach to linear response in solids” Phys. Rev. Lett., vol. 58, May. 1987, 1861-1864.
[59] X. Gonze and J.-P. Vigneron. , “Density-functional approach to nonlinear-response coefficients of solids” Phys. Rev. B, vol. 39, Jun. 1989, 13120-13128.
[60] X. Gonze, D. C. Allan, and M. P. Teter “Dielectric Tensor, EI'ective Charges, and Phonons in a-Quartz by Uariational Density-Functional Perturbation Theory” Phys. Rev. Lett., vol. 68 Jun. 1992, 3603-3606.